High Energy Physics and Nuclear Physics

Volume 21, Number 3

Temperatures and Excitation Energies of Hot Nuclei in the Reactions of $^{40}Ar+^{nat}Ag$, ^{209}Bi at 25 MeV/u

Yin Shuzhi[1], Jin Weiyang[1], Zhang Chun[1], Jin Genming[1], Zheng Jiwen[1], Wu Enjiu[1], Tan Jilian[1], Li Zuyu[1], Wang Sufang[1], Song Mingtao[1], Wu Heye[1], He Zhiyong[1], Jiang Dongxing[2], and Qian Xing[2]

[1](Institute of Modern Physics, The Chinese Academy of Sciences, Lanzhou, China)
[2](Department of Technical Physics, Beijing University)

Coincidence measurements of fission fragments and light-charged particles have been performed for the reactions of $^{40}Ar+^{nat}Ag$, ^{209}Bi at $E/A = 25$ MeV using 4 PPAC and 11 sets of $\Delta E - E$ telescopes. Angular correlations of fission fragments are plotted as a function of the folding angle between the two detected fission fragments. The linear momentum transfer distributions are derived by measured angular correlation. The backward spectra of light particles detected in coincidence with fission fragments having different average $\langle LMT \rangle$ are analyzed with a Maxwell distribution. After some corrections the initial temperature of the hot nuclei is determined from the energy spectra. The excitation energies corresponding to the different average $\langle LMT \rangle$ are obtained considering the reaction Q values and pre-equilibration emission. In the central collision of the $^{40}Ar+^{nat}Ag$, ^{209}Bi reactions, excitation energies are measured to be about 4.2 MeV/u, 2.4 MeV/u and temperatures about 6.1 MeV, 5.5 MeV, respectively. In a semi-central collision, the measured excitation energies and temperatures are about 3.5 MeV/u, 1.9 MeV/u, and 5.8 MeV, 4.8 MeV, respectively.

Key words: hot nuclei, nuclear temperature, excitation energy.

Received on August 20, 1996. Supported by the National Natural Science Foundation of China.

1. INTRODUCTION

An important area of heavy ion reaction studies is the exploration of the hot nuclei property and extreme conditions of its formation. A number of theoretical descriptions have been developed to describe properties of hot nuclei.

The possibility that nuclear phase transitions and nuclear disassembly might occur at high excitation energies has also been proposed. However, with increased excitation, energy experiments have suffered from the difficulties of experimentally isolating the hot nuclei and of determining the excitation energy and temperature of the de-exciting system.

In this experiment an angular correlation measurement and a correlation between the correlated fission fragments and light-charged particles were adopted. From analyses of these experimental data, the momentum transfer was derived by the angular correlations obtained between the fission products. The apparent temperature of the hot nuclei was inferred from the correlated light-charged particle spectra corresponding to different bins of *LMT*.

2. EXPERIMENT

The experiment was performed at HIRFL in Lanzhou. The spot of 25 MeV/u ^{40}Ar beam on target was 6×6 mm^2 and the beam current was held at about 50 nA, the ^{nat}Ag, ^{209}Bi targets were about 1 mg/cm^2 thin. The experimental setup was shown in Fig. 1. The fragment detector PPAC1 was placed at 37° to the beam direction and relative fragment detectors PPAC2, PPAC3 were placed at $-75°$, $-115°$ for the ^{209}Bi target and at $-40°$, $-60°$ for the ^{nat}Ag target. 11 sets of $\Delta E - E$ telescopes were placed around from 10° to 155°. Each set of telescope consists of two silicon ΔE detectors (50 μm +

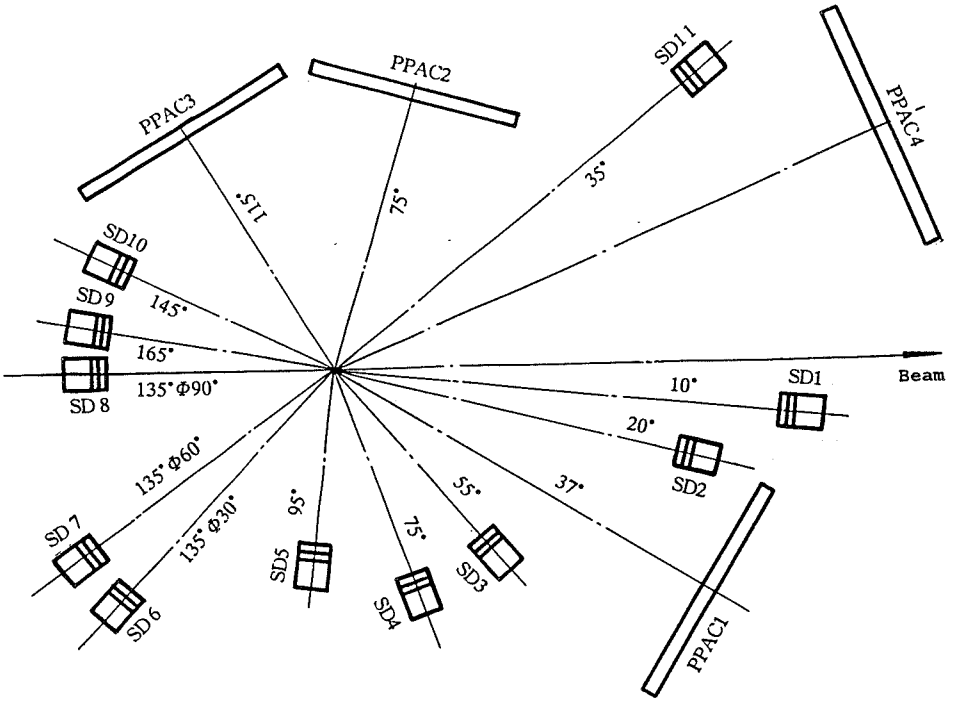

Fig. 1
Experimental setup.

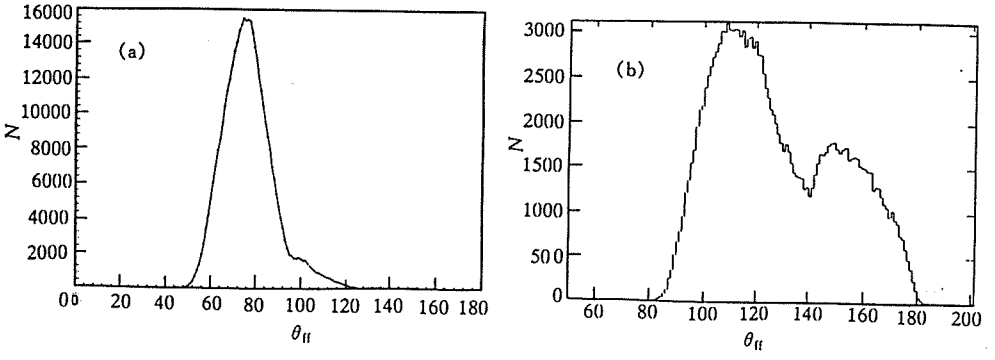

Fig. 2
Angular correlation distributions of fission fragments.
(a) $^{40}Ar+^{nat}Ag$; (b) $^{40}Ar+^{209}Bi$.

400 μm) and a CsI(Tl) scintillator with a photodiode readout E detector, which can be used for particle identification with high mass and energy resolutions. Three sets of NaI were used to measure γ rays.

The energy and time calibration of Si and the gas detector system were performed using the Thc' α source, a precision pulse-height generator, and a time calibrator. The energy calibration of the CsI(Tl) was done in separate runs, using two Si detectors in front of each CsI(Tl) detector. The energy deposited in the CsI(Tl) was determined from the observed $\Delta E_1 + \Delta E_2$ and standard range energy curves. The overall uncertainty of the energy calibrations was about 8% for the CsI(Tl) detector.

3. EXPERIMENTAL RESULTS

3.1. Angular correlations of fission fragment and linear momentum transfer

The angular correlations as a function of the folding angle θ_{ff} between the two fragments detected for the 25 MeV/u $^{40}Ar+^{nat}Ag$, ^{209}Bi reactions are shown in Fig. 2. For the ^{209}Bi target, the most probable folding angles of the central collision and the peripheral collisions are located around 115° and 155°, respectively. For the ^{nat}Ag target, the most probable folding angle central collision is located

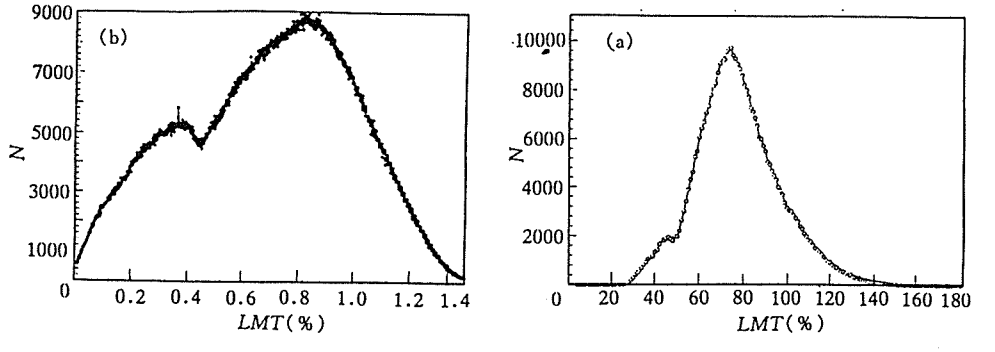

Fig. 3
The linear momentum transfer *LMT* distributions.
(a) $^{40}Ar+^{nat}Ag$; (b) $^{40}Ar+^{209}Bi$.

around 76° and no event was found which came from peripheral collision. The linear momentum transfer distributions were derived by measured angular correlations and shown in Fig. 3. The primary composite nuclei velocities were obtained by fragment kinematics

$$v_{cn} = \frac{v_1 v_2 \sin(\theta_1 + \theta_2)}{v_1 \sin\theta_1 + v_2 \sin\theta_2} \quad . \tag{1}$$

In this experiment, the fragment velocities cannot be determined well because counts coming from NaI are too small. We assume that most of fragments are coming from symmetric fissions and velocities of two fragments in the center of mass are equal about 1.2 cm/ns. Thus, the velocity of the compound nuclei is given as follows:

$$v_{cn} = \frac{v_{1c}}{\sqrt{1 + \dfrac{\sin^2\theta_2}{\sin^2(\theta_1 + \theta_2)} - \dfrac{4\sin\theta_2 \cos\theta_1}{\sin(\theta_1 + \theta_2)}}} \tag{2}$$

and the linear momentum transfer is

$$LMT = \frac{A_t}{A_p} \frac{v_{cn}}{(v_p - v_{cn})} \quad , \tag{3}$$

where A_p and A_t are the projectile and target mass, and v_p is the projectile velocity. In Fig. 3, the *LMT* distribution shows a gaussian shape. The probable linear momentum transfer $\langle LMT \rangle$ for ^{nat}Ag and ^{209}Bi targets are 0.76 and 0.8, respectively. Viola's [1] linear momentum transfer systematic gives

$$\frac{d^2\sigma}{d\Omega dE} = \frac{N}{2(\pi T)^{3/2}} (E - B_C)^{1/2} \times \exp[-(E - B_C)/T], \tag{4}$$

For 25 MeV/u ^{40}Ar beam, the calculated value by Eq.(4) is 0.813; it agrees with the experimental results of ^{209}Bi target and is larger than that of ^{nat}Ag target. For ^{nat}Ag target the *LMT* distribution shows a central collision component and no peripheral component is found. However, the latter phenomenon needs further experimental confirmation.

3.2. Temperature and excitation energies of the primary residues

The energy distribution of emitted light particles in the source rest frame is given by [2]

$$\frac{d^2\sigma}{d\Omega dE} = \frac{N}{4\pi T^2} (E - B_C) \times \exp[-(E - B_C)/T], \tag{5}$$

for a surface emission and

$$\langle LMT \rangle = 1.273 - 0.092\sqrt{E/A} \quad . \tag{6}$$

for a volume emission. Here T is the source temperature and B_c is the minimum coulomb energy of particle. N is normalization factor, E is the particle energy in the emission frame. The pre-equilibrium light particles are emitted mainly in the forward direction and equilibrium light particles are emitted isotropically, so the temperature obtained from backward light particle energy spectra is the temperature after system equilibration.

Table 1
LMT, excitation energies, and temperatures.

Target	*LMT* Window	E^*/u(MeV)	Particle	θ	T_{app} (MeV)	T_{int} (MeV)
Ag	0.50 – 0.75	3.5	α	95°	5.32 ± 0.36	5.81 ± 0.39
	0.75 – 1.00	3.5	α	115°	5.29 ± 0.48	5.78 ± 0.52
	0.75 – 1.00	4.2	α	95°	5.59 ± 0.55	6.10 ± 0.60
	0 – 0.33	4,2	α	115°	5.51 ± 0.47	6.02 ± 0.51
	0.33 – 0.66	2.1	p	95°	4.13 ± 0.39	4.51 ± 0.43
	0.66 – 1.00	3.0	p	95°	5.00 ± 0.31	5.48 ± 0.34
	0.50 – 0.75	4.02	p	95°	5.29 ± 0.23	5.78 ± 0.25
Bi	0.40 – 0.75	1.88	α	155°	4.34 ± 0.27	4.77 ± 0.29
	0.75 – 1.00	2.40	α	155°	4.96 ± 0.28	5.46 ± 0.30

The backward spectra of light particle detected in coincidence with fission fragment having different average $\langle LMT \rangle$ are analyzed with a Maxwell distribution. Initial temperatures of the hot nuclei are determined from the energy spectra. The emission process is sequential evaporation, with equilibrium re-established after each emission, light particles could by emitted at various excitation energies during the de-excitation cascade and the observed temperatures T_{app} would be weighted averages over the entire cascade. Nearly all light particles coming from the correlated fission fragments have been assumed. The light particle spectra of laboratory system were transformed into the center of mass system. The initial temperature is given by $\langle T_{int} \rangle = (r_2T_2 - r_1T_1)/(r_2 - r_1)$, where T_1 and T_2 represent the apparent temperatures of excitation energies E_1 and E_2, respectively. r_1 and r_2 are corresponding multiplicities. The initial temperatures, apparent temperatures, and excitation energy in this work are shown in Table 1.

In the cluster transfer frame, the excitation energy of the residual system is given by:

$$E^* = \frac{m_t}{m_p + m_t / \langle LMT \rangle} E_{lab} + Q + E_{rod} \ , \tag{7}$$

where m_p, m_t, E_{lab}, and Q are the mass of the projectile, target, the incident energy, and the reaction Q value, respectively. E_{rod} is the rotational energies of the residue nuclei. Assuming transferred nuclear

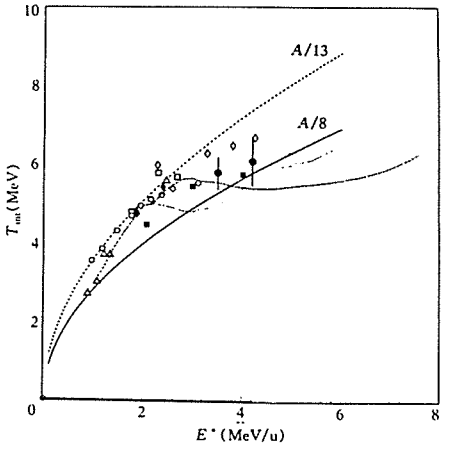

Fig. 4
Initial temperatures and excitation energies.
Δ: N+Sm; ◇: S+Ag; □: O+Ag; ○: Ar+Au; ●: Ar+Ag(α); ■: Ar+Ag(p); ♦: Ar+Bi(α).
–·–·–: Bondorf A = 100 [3], ·····: Gross Xe (A = 13) [14].

number $m_{tr} = \langle LMT \rangle \times m_p$ and the residual nuclear number $m_{cn} = m_t + m_{tr}$, neglecting some corrections of reaction Q value and rotational energies E_{rod}, the excitation energies uncertainty is less than 8%.

4. DISCUSSION

The excitation energies and initial temperatures derived in this work are plotted in Fig. 4 with data of the $^{14}N+^{154}Sm$ reactions at 19 and 35 MeV/u [5] and 30 MeV/u ^{16}O, ^{32}S on ^{nat}Ag [6], 25 MeV/u $^{40}Ar+^{197}Au$ [7].

In the range of excitation energies below 1 MeV/u, the level density parameter a, which is defined by the low-energy Fermi gas approximation as $E^* = aT^2$, is approximately equal to $A/8$. In the excitation energy range between 1 and 3 MeV/u, a decreases to $A/13$. Above 3 MeV/u a value tends to increase again. Our experimental results approached $A/8$. Initial temperatures are lower because of lower statistics of light particle spectra and fewer bins of LMT which result in a stronger average effect of excitation energies. On the other hand, only most of the excitation energies are transferred into thermal excitation energies and pre-equilibrium light particles carry away part of excitation energies so that experimental results have some uncertainties.

REFERENCES

[1] V.E. Viola, *Phys. Rev.*, **C31**(1985), p. 1550.
[2] A.S. Goddhaber, *Phys. Rev.*, **C17**(1978), p. 2247.
[3] J. Bondorf *et al.*, *Nucl. Phys.*, **A444**(1985), p. 460.
[4] D. Gross, *Phys. Rev. Lett.*, **56**(1986), p. 1544.
[5] K. Hagel *et al.*, *Nucl. Phys.*, **A486**(1988), p. 429.
[6] D. Fabris *et al.*, *Phys. Lett.*, **B196**(1987), p. 429.
[7] Wu Heyu *et al.*, *IMP Annual Report*, (1993), p. 12.